

Supporting Information

CRISPR-Cas12a Nucleases Bind Flexible DNA Duplexes without RNA-DNA Complementarity

Wei Jiang¹, Jaideep Singh¹, Aleique Allen¹, Yue Li¹, Venkatesan Kathiresan¹, Omair Qureshi¹, Narin Tangprasertchai^{1,‡}, Xiaojun Zhang¹, Hari Priya Parameshwaran³, Rakhi Rajan³, and Peter Z. Qin^{1,2,*}

¹Department of Chemistry and ²Department of Biological Sciences, University of Southern California, Los Angeles, CA 90089, USA

³Department of Chemistry and Biochemistry, Price Family Foundation Institute of Structural Biology, Stephenson Life Sciences Research Center, University of Oklahoma, Norman, OK, 73019, USA

‡Present Addresses: GenapSys, Inc., 200 Cardinal Way, Redwood City, CA 94063

*Corresponding author: Peter Z. Qin, 3430 S. Vermont Ave., Los Angeles, CA 90089, USA;
Tel: (213) 821-2461; Fax: (213) 740-2701; Email: pzq@usc.edu

Table of Contents

- S1: Additional information on crRNAs
- S2: Additional information on substrate DNA constructs
- S3: Cleavage of cognate DNA substrates
- S4: Cleavage of DNA substrate requires crRNA
- S5: Assessing the impact of MBP-tag on LbCas12a activities
- S6: Non-target strand cleavage with LbRNA-a
- S7: Comparison of DNA cleavage with LbRNA-a and LbRNA-b
- S8: Assessing non-specific trans-cleavage activity
- S9: Additional data obtained with the competition assay
- S10: DNA binding assessed by a native gel shift assay
- S11: Flexibility of DNA duplexes assessed by site-directed spin labeling

S1. Additional information on crRNAs

The full sequences of the crRNAs are listed in Table S1, and the corresponding DNA templates for T7 *in vitro* transcription are listed in Table S2. Each crRNA contained an ortholog-specific repeat sequence followed by a 3' 24-nucleotide single-stranded segment. The 5' first 20-nucleotide of the single-stranded segment was the RNA-guide (underlined in Table S1).^{1,2} The remaining 4 nucleotides would not hybridize with the DNA and were disordered in reported crystal structures.¹ These 4 extra nucleotides did not interfere with investigations of DNA duplex cleavage,² but mitigated potential problems arising from inhomogeneity in the 3'-terminus of T7-transcribed RNAs.

Table S1. Sequences of crRNAs

Name	Sequence (5'-3') ^(a)
LbRNA-a	GGAAUUUCUACUAAGUGUAGAU <u>GACAGCCCACAUGGCAUCCACUU</u>
LbRNA-b	GGAAUUUCUACUAAGUGUAGAU <u>AGUGACAUGUGCAGUGCCGUGUCC</u>
AsRNA-a	GGAAUUUCUACU-CUUGUAGAU <u>GACAGCCCACAUGGCAUCCACUU</u>
AsRNA-b	GGAAUUUCUACU-CUUGUAGAU <u>AGUGACAUGUGCAGUGCCGUGUCC</u>
FnRNA-a	GGAAUUUCUACU-GUUGUAGAU <u>GACAGCCCACAUGGCAUCCACUU</u>

(a) RNA guides are underlined. The RNA-a sequence is shown in blue, and the RNA-b guide sequence is shown in green.

Table S2. DNA templates used for T7 *in vitro* transcription

Name	Sequence (5'-3') ^(a)
LbRNA-a template	AAGTGGAAATGCCATGTGGGCTGTCATCTACTTAGTAGAAATTCcta tagtgagtcgtattag
LbRNA-b template	GGACACGGCACTGCACATGTCACTATCTACTTAGTAGAAATTCcta tagtgagtcgtattag
AsRNA-a template	AAGTGGAAATGCCATGTGGGCTGTCATCTACAAGAGTAGAAATTCctat agtgagtcgtattag
AsRNA-b template	GGACACGGCACTGCACATGTCACTATCTACAAGAGTAGAAATTCctat agtgagtcgtattag
FnRNA-a template	AAGTGGAAATGCCATGTGGGCTGTCATCTACAACAGTAGAAATTCctat agtgagtcgtattag
T7 top-strand	CTAATACGACTCACTATAG

(a) Lower case letters indicate the segment that hybridizes with the "T7 top-strand" to form the T7 promoter.

S2. Additional information on substrate DNA constructs

A target DNA duplex consisted of a central variable region flanked by a PAM at one end and two additional constant segments (Figure S1). The strand containing the sequence complementing the RNA guide was designated as the target-strand (t-strand), while the other strand was designated as the non-target strand (nt-strand). Referencing to the nt-strand, the sequences of the constant segments were: PAM, 5'-TTTC-3'; PAM-proximal, 5'-TTCCACTCGCTCAA-3'; and PAM-distal: 5'-ATCACTGGCATCC-3'.

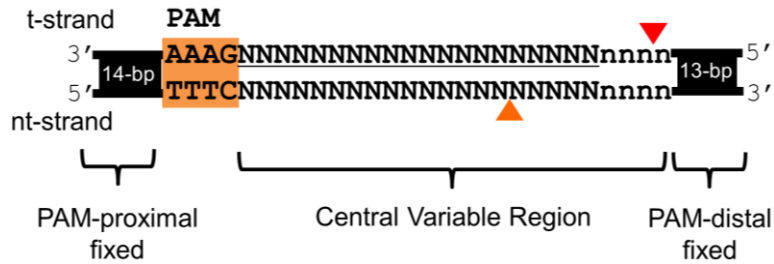


Figure S1. Schematic of the DNA duplexes used in this work. The PAM is highlighted with orange. The two wedges indicate observed DNA cleavage sites. The underlined segment at the t-strand complemented the RNA guide.

The sequences of the central variable region were listed in Table S3. Note that the length of the segment was designed as 24-nucleotide (-nt) based on the initial report on Cas12a.² Later studies revealed that only the 20-nt PAM-proximal sequence (Figure S1, underlined) acts as the protospacer and forms base-pairing with the RNA guide.¹

Table S3. List of variable sequences in the DNA duplexes

Name	Sequence ^(a,b,c)	Extinction Coefficient (M ⁻¹ ·cm ⁻¹)	
		t-strand ^(d)	nt-strand ^(d)
i	3' - <u>CTGTCGGGTGTACCGTAAGGTGAA</u> - 5' 5' - GACAGCCACATGGCATTCCACTT - 3'	554,200	495,500
ii	3' - <u>ctgtcGggtgtacCgtaaggtgaa</u> - 5' 5' - agtgaCatgtgcaGtgccgtgtcc - 3'	554,200	500,000
iii	3' - <u>tcactGtacacgtCacggcacagg</u> - 5' 5' - gacagCccacatgGcattccactt - 3'	545,900	495,500
iv	3' - <u>TCACTGTACACGTCACGGCACAGG</u> - 5' 5' - AGTGACATGTGCAGTGCCGTGTCC - 3'	545,900	500,000
v	3' - <u>tCACTGTACACGTCACGGCACAGG</u> - 5' 5' - gGTGACATGTGCAGTGCCGTGTCC - 3'	545,900	497,300
vi	3' - <u>tcACTGTACACGTCACGGCACAGG</u> - 5' 5' - gaTGACATGTGCAGTGCCGTGTCC - 3'	545,900	499,800
vii	3' - <u>tcaCTGTACACGTCACGGCACAGG</u> - 5' 5' - gacGACATGTGCAGTGCCGTGTCC - 3'	545,900	498,500
viii	3' - <u>tcacTGTACACGTCACGGCACAGG</u> - 5' 5' - gacaACATGTGCAGTGCCGTGTCC - 3'	545,900	500,000

(a) The t-strand is shown on the top in the 3' to 5' direction, and the nt-strand is shown at the bottom in the 5' to 3' direction.

(b) The 20-nt protospacer is underlined.

(c) Paired nucleotides are shown in upper case letters, and unpaired nucleotides are shown in lower case letters.

(d) Extinction coefficients are listed for the entire 55-nt DNA strand.

S3: Cleavage of cognate DNA substrates

Figure S2 shows results of DNA duplex i (Table S3) cleavage by Cas12a effectors containing the RNA-a guide (Table S1). Analyses showed that the t-strand cleavage yielded predominately a 13-14 nucleotide 5' fragment, corresponding to a cleavage site located 23-24 nucleotides from the PAM as previously reported.² Cleavage of the nt-strand produced a 32-nucleotide 5' fragment, corresponding to a cleavage site located 14-nucleotide from the PAM. Both t- and nt-strand cleavage sites fall in the same range as reported from a number of Cas12a studies,^{2,4} resulting in sticky-end products as expected.²

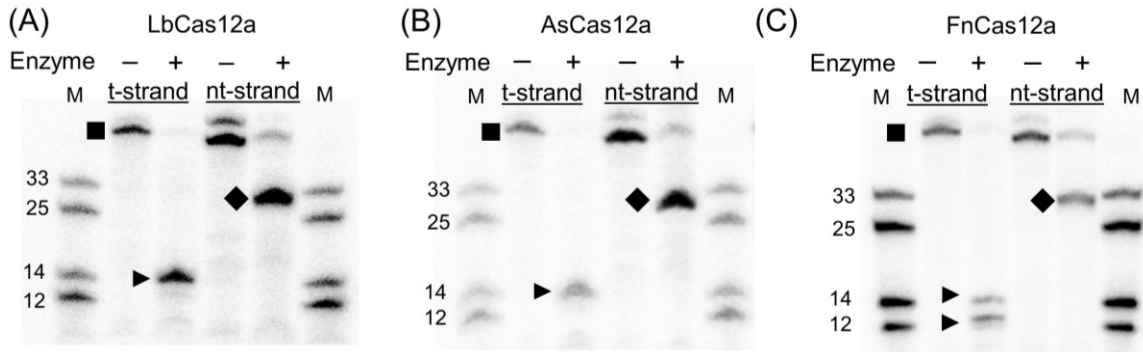


Figure S2: Reconstituting the Cas12a enzyme. Representative denaturing gels showing cleavage of the cognate duplex i (1 nM) by effectors (10 nM) of (A) LbCas12a/LbRNA-a; (B) AsCas12a/AsRNA-a; and (C) FnCas12a/FnRNA-a. Reactions were monitored with 5'-³²P labeled t- or nt-strand as indicated. Precursors are marked by "■", products of t- and nt-strand are marked by "▶" and "◆", respectively. Size of DNA products were obtained by comparing with the DNA size marker (M). Note that control experiments (data not shown) indicated that the presence of two precursor bands was the result of incomplete DNA duplex denaturation, with the upper precursor band being the duplex and the lower one being the single strands.

S4. Cleavage of DNA substrate requires crRNA

DNA duplex **i** was incubated with Cas12a proteins in the absence of crRNA (Figure S3). No cleavage product was observed, indicating that DNA cleavage requires crRNA.

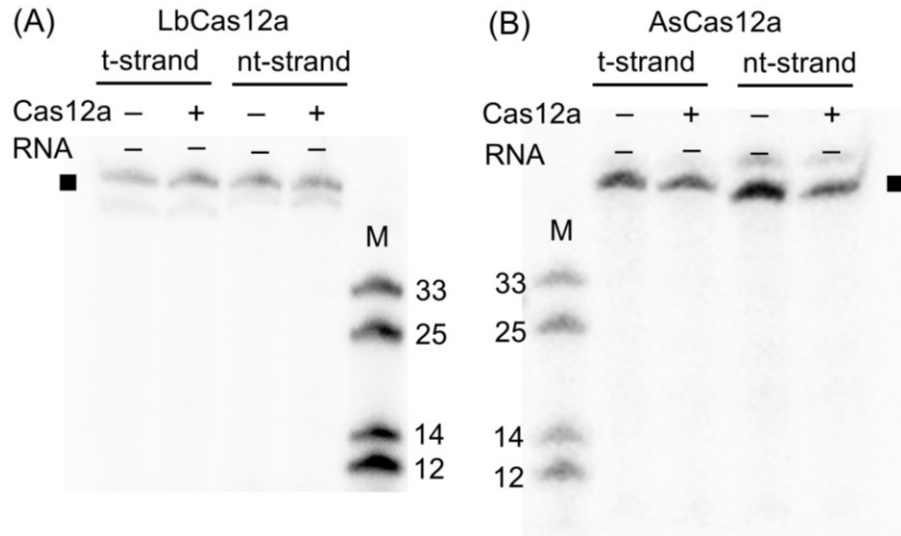


Figure S3: Examples of autoradiographs of DNA duplex **i** incubated with proteins of (A) LbCas12a and (B) AsCas12a. DNA precursors (marked by "■") were ^{32}P -labeled on either the t-strand or the nt-strand. Data shown were obtained with 10 nM DNA duplex and 100 nM Cas12a protein in the absence of crRNA. No cleavage product was observed, indicating that DNA cleavage requires crRNA.

S5. Assessing the impact of MBP-tag on LbCas12a activities

Control experiments were carried out using LbCas12a protein with an N-terminal MBP tag. As shown in Figure S4, the data indicated that the MBP tag has no effect on results obtained with the cleavage and competition assays reported in this work.

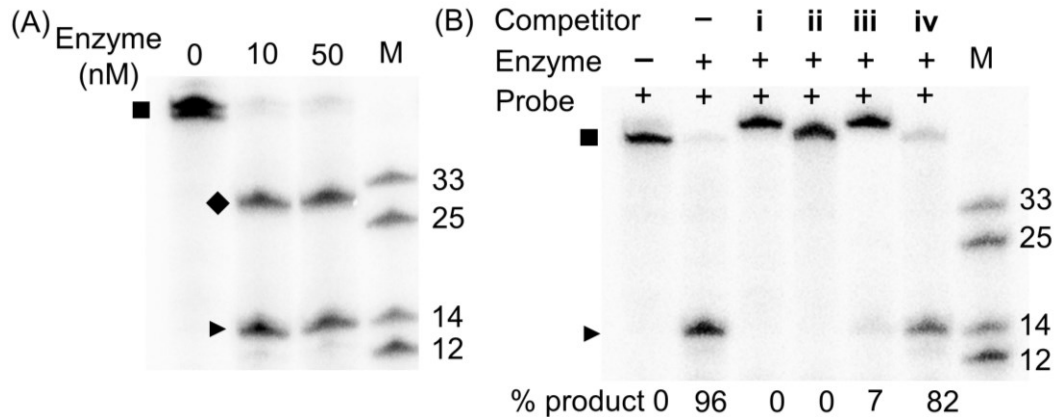


Figure S4. (A) Cleavage assay with DNA duplex i. Data shown were obtained with 1 nM duplex i labeled with ^{32}P at both strands and various concentrations of tagged LbCas12a complexed with LbRNA-a. Both DNA strands were cleaved in the same fashion as observed for LbCas12a without the tag (Figure S2A). (B) Competition assay with signal derived from ^{32}P -labeled DNA duplex i*. Data shown were obtained with 1 nM t-strand labeled duplex i*, 10 nM enzyme (i.e., tagged LbCas12a complexed with LbRNA-a), and 1 μM unlabeled competitor DNAs. The results show the same pattern as that observed for LbCas12a without tag (Main Text, Figure 2C).

S6. Non-target strand cleavage with LbRNA-a guided effector

DNA cleavage was measured using an effector complex of LbCas12a/LbRNA-a. As shown in Figure S5, cleavage of the non-target strand (nt-strand) was observed for duplexes **i** and **ii**, in which the protospacer complements the guide of LbRNA-a. No cleavage was observed for either **iii** or **iv**, in which the protospacer largely lacks complementarity to the LbRNA-a guide. The data showed that complementarity between the DNA protospacer and RNA guide is required for nt-strand cleavage.

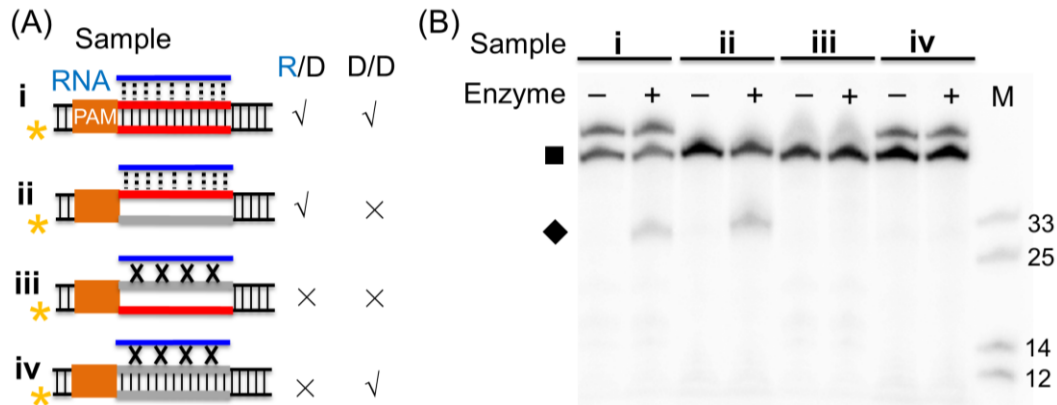


Figure S5: (A) Schematic of DNA duplexes. “*” marks the ³²P-label on the nt-strand. The guide strand of RNA-a is represented by the blue line, the DNA protospacer is shown in red, and the PAM is highlighted in orange. Pairings between the DNA strands are indicated by solid vertical lines. Complementarity between the RNA guide and the DNA target strand is indicated by dashed vertical lines, and the lack of complementarity between RNA and DNA is indicated by crossed lines. The relationships between the RNA-guide and protospacer t-strand (R/D) and protospacer t- and nt-strand (D/D) are indicated on the right. (B) Autoradiograph with signal derived from ³²P-labeled nt-strand. Data were obtained with 10 nM LbCas12a/LbRNA-a complex (i.e., the “enzyme”) and 1 nM DNA duplexes.

S7. Comparison of DNA cleavage with LbRNA-a and LbRNA-b

Control experiments were carried out with crRNAs that differ in their guides. As expected, duplexes were only cleaved if its protospacer t-strand matched the corresponding RNA guide. The data confirmed that complementarity between the RNA guide and the t-strand of the DNA protospacer is required for cleavage.

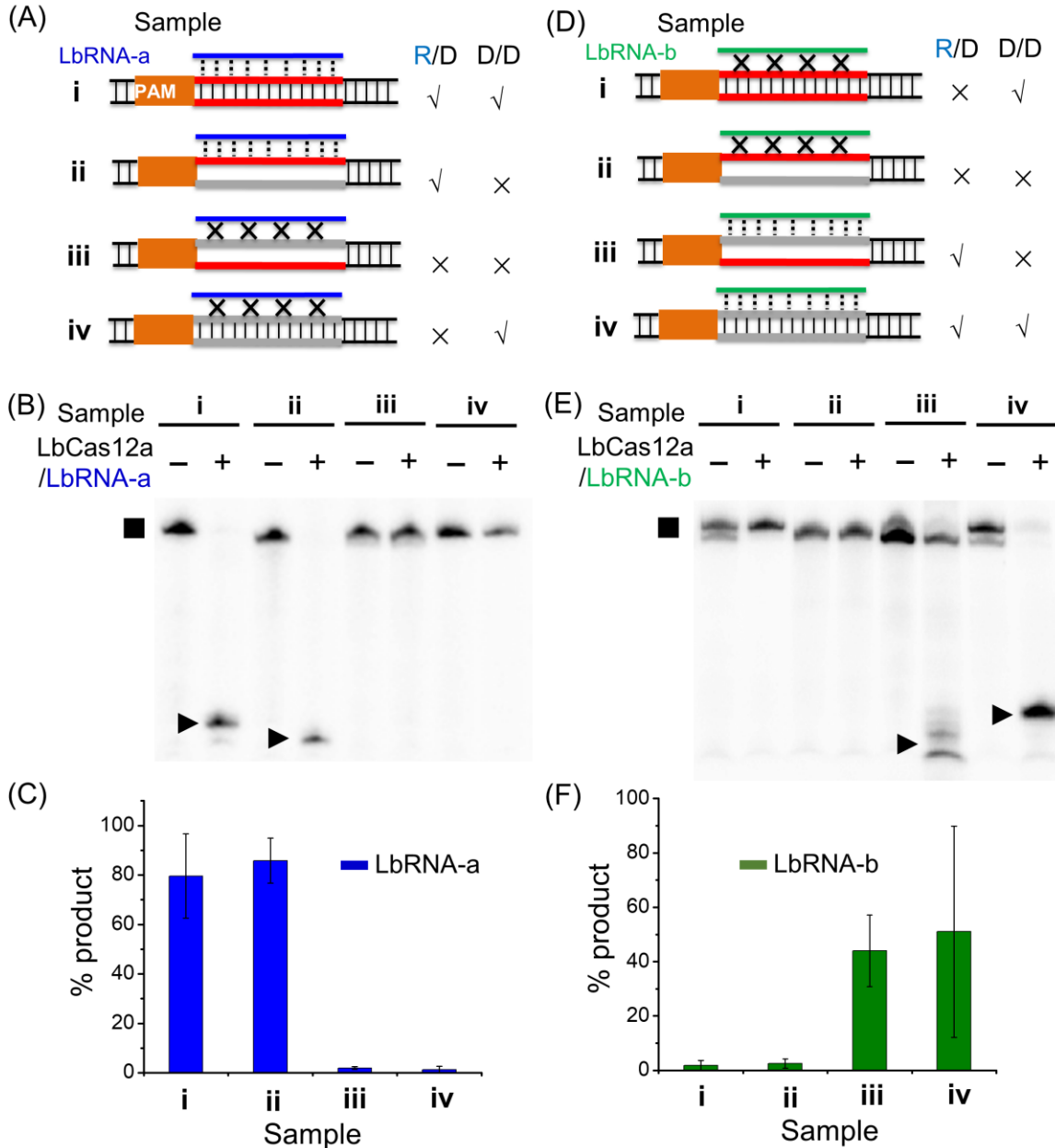


Figure S6. DNA cleavage with different RNA guides. (A) and (D) show schematics of nucleic acid constructs, with pairings between the DNA strands indicated by solid vertical lines, and complementarity between the RNA guide (blue for LbRNA-a and green for LbRNA-b) and the protospacer t-strand indicated by dashed vertical lines. The relationships between the RNA-guide and protospacer t-strand (R/D) and protospacer t- and nt-strand (D/D) are indicated on the right. (B) and (E) show examples of cleavage of 10 nM DNA by 100 nM LbCas12a/RNA complex, with the signals derived from ³²P-labeled t-strand. Panel (B) is the same as that shown in main text Figure 1C. (C) and (F) show plots quantitating the percentages of the t-product for duplexes i to iv.

S8. Assessing non-specific trans-cleavage activity

Figure S7 shows results of an experiment assessing *trans-cleavage* of duplex **iii**, which has the majority of the protospacer unpaired (Table S3). When the LbCas12a effector was activated by the cognate substrate duplex **i**, as expected the single-stranded DNA controls were cleaved non-specifically (Figure S7, ss-1 and ss-2). Very little cleavage was observed for duplex **iii**. The data demonstrated that under experimental conditions used in the present work, a bubble DNA with “single-stranded” region in the protospacer is not a trans-cleavage target.

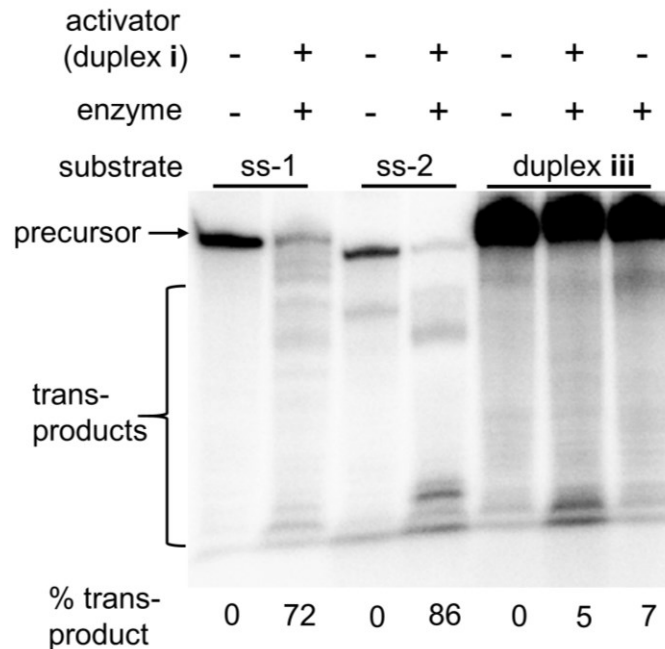


Figure S7. A representative gel showing trans-cleavage results. Data shown were obtained with 10 nM ³²P-labeled substrate and 100 nM LbCas12a/LbRNA-a complex activated by 100 nM unlabeled cognate duplex DNA **i**. The activator DNA duplex was assembled with Cas12a/RNA effector in the cleavage reaction buffer following procedures described in Methods (i.e., “DNA cleavage assay”). The ³²P-labeled substrate was then incubated with the Cas12a effector/activator complex at 37°C for 30 minutes. The reaction was quenched and resolved by denaturing PAGE. The trans-cleavage results were visualized and quantified by autoradiography. The %trans-product shown was corrected for DNA degradations in the absence of enzyme. The sequences of the control single-stranded DNAs are: ss-1, 5'-TTCCACTCGCTCAATTTTCGACAGCCCACATGGCATTCCACTTATCACTGGCATCC-3'; ss-2, 5'-AAAAAAAAAGTCGTCGCTTTTTTTTTTTTTTTTTTTTGTGCTGTTAAAAAAAA-3'. The substrate duplex **iii** was ³²P-labeled on both strands.

S9. Additional data obtained with the competition assay

S9a: Quantification of Competition Results

Tables S4 and S5 show the amount of product obtained in the presence of various competitors. The data shown were obtained with 1 nM i* (³²P-labeled t-strand), 10 nM effector, and 1 μM competitor (these conditions were used to obtain the representative gels shown in Figures 2 and 3 of the main text). The data were reported as “Average ± Standard Deviation” from at least three repetitions. A competitor allowing a lower percentage of product inhibits the enzyme more effectively, thus binds to the enzyme with a higher affinity.

TABLE S4. DNA i* cleavage by effectors guided with RNA-a in the presence of competitor duplex i – iv

Competitor	% product	
	LbCas12a	AsCas12a
none	72 ± 29	64 ± 27
i	2 ± 2	0 ± 0
ii	1 ± 2	0 ± 0
iii	11 ± 5	1 ± 2
iv	88 ± 4	65 ± 11

TABLE S5. DNA i* cleavage by effectors guided with RNA-a in the presence of competitor duplex iv – viii

Competitor	Bubble size (bp)	% product	
		LbCas12a	AsCas12a
none		77 ± 19	72 ± 3
iv	0	55 ± 16	45 ± 15
v	1	53 ± 17	13 ± 5
vi	2	38 ± 14	4 ± 0
vii	3	30 ± 19	2 ± 2
viii	4	8 ± 4	2 ± 2

S9b. Competition carried out with FnCas12a

Figure S8 shows competition results obtained with a catalytically-active FnCas12a/FnRNA-a effector, which has the same pattern as those observed from Lb- and AsCas12a effectors (Main text, Figure 2). Duplexes **i** and **ii** maintained complementarity between the protospacer t-strand and the RNA-a guide, and as expected competed for probe binding and completely inhibited cleavage. Duplexes **iii** and **iv** inhibited probe cleavage to a less extent as compared to that of **i** and **ii** because they largely lacked RNA-guide/t-strand complementarity. Importantly, duplex **iii**, which has unpaired DNA t-/nt-strand, gave less cleavage product than that of duplex **iv**, which has fully-paired t-/nt-strand, indicating duplex **iii** bound to the FnCas12a effector with a higher affinity. Also note that the difference between duplexes **iii** and **iv** was smaller than that observed for Lb- and AsCas12a (Table S4). This may suggest differences between Cas12a orthologs in binding flexible DNAs. This will be an interesting subject for future investigations.

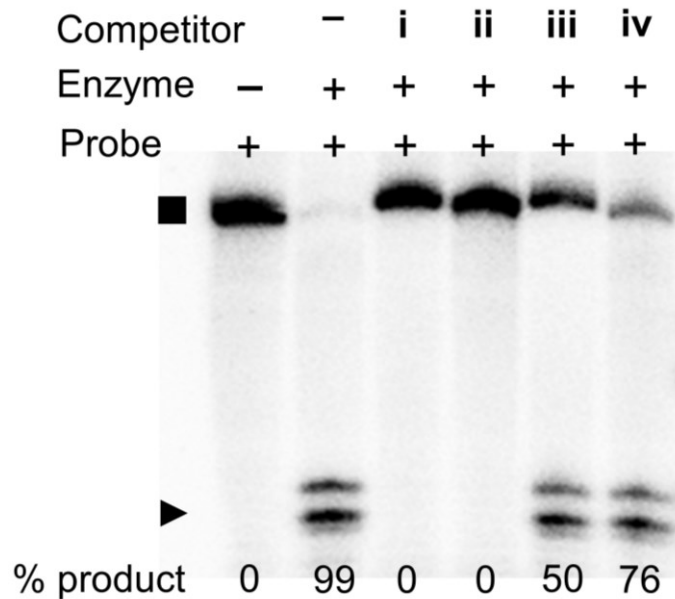


Figure S8. A denaturing gel showing competition results with FnCas12a. Data were obtained with 1 nM substrate **i*** with ^{32}P -labeled t-strand, 10 nM FnCas12a/FnRNA-a complex, and 1 μM competitor DNA (substrate **i-iv**, unlabeled). Precursors are marked by “■” and t-strand products by “▶”.

S9c. Competition carried out with 100 nM enzyme complex

Competition experiments were carried out with 100 nM Cas12a enzyme (Figure S9). For both Lb- (Figure S9B) and AsCas12a (Figure S9C) complexed with RNA-a, competitor **iii** reduces the amount of products as compared to **iv**, indicating that **iii** has a stronger ability to bind to the Cas12a. As expected, with a larger amount of enzyme available to interact with various DNAs, the differences between **iii** and **iv** are reduced as compared to those observed with 10 nM Cas12a enzyme (main text Figure 2).

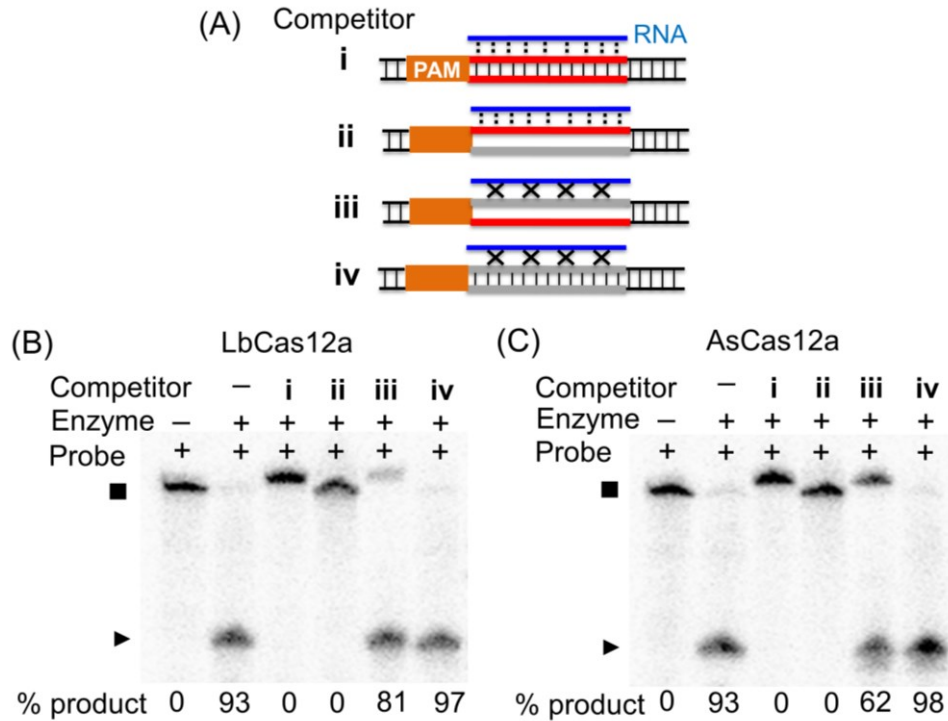


Figure S9: Competition with 100 nM Cas12a enzyme. (A) Schematics of the competitor duplexes. (B) Results obtained with LbCas12a/LbRNA-a. (C) Results obtained with AsCas12a/AsRNA-a. Data shown were obtained with 1 nM duplex precursor **i*** (³²P labeled t-strand), 1 μM unlabeled competitor DNA, and 100 nM enzyme complex.

S9d. Effects of PAM

To assess the role of the PAM in this work, the PAM of duplex **iii** was altered to generate a PAM-less duplex **ix** (Figure S10A). Competitions were carried out using LbCas12a/LbRNA-a as the enzyme and its cognate substrate duplex **i** as the probe. The results (Figure S10B) showed that duplex **iii** clearly competes better than duplex **ix**, thus binding to Cas12a with a higher affinity. Both duplexes **iii** and **ix** have unpaired DNA protospacer and largely lack complementarity to the RNA-a guide. The data demonstrated that as expected a proper PAM contributes to Cas12a binding to DNA duplexes. Also note that duplex **ix**, which has a flexible protospacer but without a proper PAM, still binds better than duplex **iv**, which has a rigid protospacer and a proper PAM. While this work focused on PAM-containing DNA duplexes, detailed investigation on impacts of altering PAM may be an interesting subject for future studies.

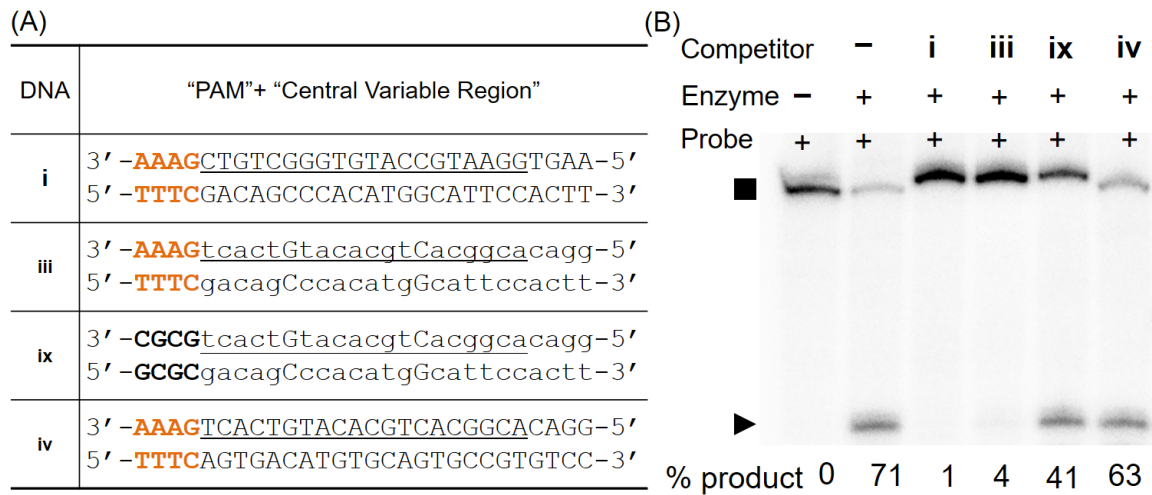


Figure S10. Assessing effects of PAM. (A) DNA duplexes. Sequences of the PAM and Central-Variable-Region are shown, while the invariant PAM-proximal and PAM-distal segments (Sect. S2) are omitted. Upper case letters indicate paired nucleotides, and lower case letters indicate the unpaired nucleotides. The duplex segment regarded as "PAM" is shown in bold, and the 20-nucleotide protospacer is underlined. (B) An example of a gel showing competition results. Data were obtained with 1 nM substrate **i*** with ³²P-labeled t-strand as probe, 10 nM LbCas12a/LbRNA-a complex, and 1 μM competitor DNA.

S9e: Competition carried out with LbCas12a/LbRNA-b complex

Figure S11 shows competition results obtained with an LbCas12a/LbRNA-b effector, with the RNA guide complementing the protospacer t-strand in duplexes **iii** and **iv**. Cleavage of substrate **iv*** was observed in the presence of competitor **i** but was greatly reduced with **ii**, indicating **ii** has a much higher degree of binding to Cas12a. Neither **i** nor **ii** complements the LbRNA-b guide, but the two duplexes differ in the protospacer: **ii** contains large bubbles and **i** is fully-paired. With the bubbles, duplex **ii** has a high flexibility, which allows binding to Cas12a.

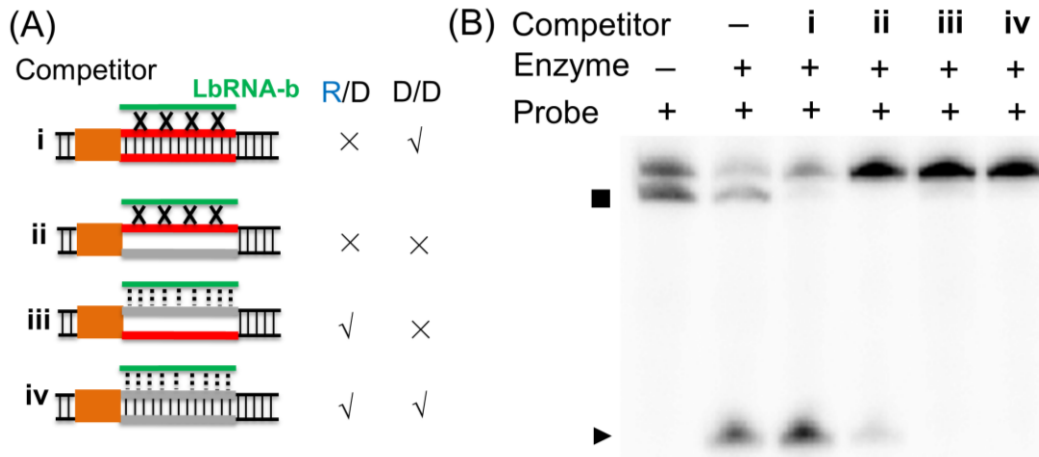


Figure S11. (A) Schematic of the assay. The guide of RNA-b is shown in green, the DNA protospacer segment is indicated by colored lines. Pairing between the DNA strands is indicated by solid vertical lines, and complementarity between the RNA guide and the protospacer t-strand is indicated by dashed vertical lines. The relationships between the RNA-guide and protospacer t-strand (R/D) and protospacer t- and nt-strand (D/D) are indicated on the right. (B) An example of a gel showing competition results. Data were obtained with 1 nM substrate **iv*** with ³²P-labeled t-strand, 10 nM LbCas12a/LbRNA-b complex, and 1 μM competitor DNA (substrate **i-iv**, unlabeled).

S9f: Competition with duplexes containing completely unpaired protospacer

In duplexes **ii** and **iii** (Table S3), the protospacer t- and nt-strand have individual complementary nucleotides at the 6th and 14th positions from the PAM. These PAM-distal complementary nucleotides are separated by 7 unpaired nucleotides, therefore do not provide sufficient interaction to support t-/nt-strand pairing within the 20-nt protospacer. To further confirm that the individual complementary nucleotides do not impact conclusions drawn from data obtained using duplexes **ii** and **iii**, competition experiments were carried out using DNA duplexes **ii'** and **iii'**, which completely eliminated complementarity among the protospacer t- and nt-strand (Figure S12A). The results were indeed the same as those obtained from duplexes **ii** and **iii** (Figure S12B). This indicates that further “enhancing” the flexibility of the protospacer by completely removing t- and nt-strand pairing has little impact on off-target binding to the Cas12a active site.

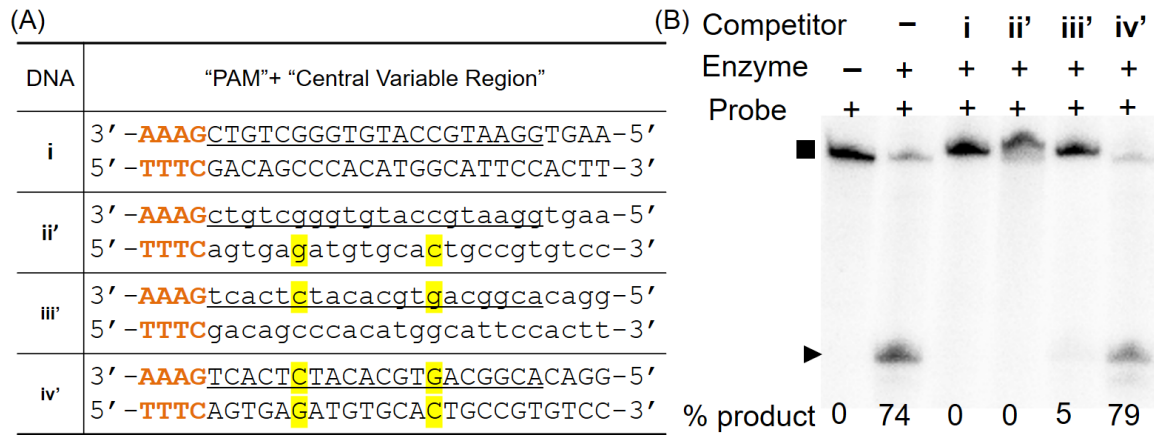


Figure S12. Competition with duplexes containing completely unpaired protospacer. (A) DNA duplexes. Sequences of the PAM and Central-Variable-Region are shown, while the invariant PAM-proximal and PAM-distal segments (Sect. S2) are omitted. Upper case letters indicate paired nucleotides, and lower case letters indicate the unpaired nucleotides. The duplex segment regarded as “PAM” is shown in orange bold, and the 20-nucleotide protospacer is underlined. Highlighted in yellow are differences between these constructs to duplex **ii**, **iii**, and **iv** shown in Table S3. (B) An example of a gel showing competition results. Data shown were obtained with 1 nM substrate **i*** with ³²P-labeled t-strand, 10 nM LbCas12a/LbRNA-a complex, and 1 μM competitor DNA (unlabeled). Duplexes **i** and **ii'** maintained full complementarity between the protospacer t-strand and the RNA-a, and bound to Cas12a and prevented probe cleavage. Duplexes **iii'** and **vi'** lacked any complementarity between the protospacer t-strand and the RNA-a guide. Duplex **vi'** allowed similar amount of product as observed in the absence of competitor, indicating it did not bind to the Cas12a. Duplex **iii'** allowed very little product formation, similar to that observed for duplex **iii** (Table S4). This indicates that **iii'** and **iii** are equivalent in inhibiting cleavage, and bind to Cas12a in a similar fashion.

S10. DNA binding assessed by a native gel shift assay

Figure S13 shows the results of a native gel shift measurement using a catalytically in-active binary dFnCas12a/FnRNA-a effector complex. The on-target duplex **i** was completely bound at 100 nM effector. Duplex **iii**, which has an unpaired DNA protospacer and largely lacks complementarity between the protospacer t-strand and RNA-a guide, showed weak binding at 100 nM effector, but was bound nearly completely at 1000 nM. Duplex **iv**, which has a fully-paired DNA protospacer but largely lacks complementarity between the protospacer t-strand and RNA-a guide, showed no binding at 100 nM effector and little binding at 1000 nM. The data indicated that the off-target flexible duplex (i.e., **iii**) binds with a higher affinity to the binary Cas12a effector complex as compared to the fully-paired rigid off-target duplex (i.e., **iv**).

Also note that in a Cas12a study by Singh and co-workers,⁵ at effector concentrations of 100 -- 300 nM, no apparent binding was detected with DNAs containing PAM-adjacent mismatch bubble of 2 and 4 base-pairs. The Singh study included little characterization on binding of these bubble DNAs. In our work the bubble-containing duplex **iii** showed low but detectable binding with 100 nM effector. The discrepancy likely arises due to minor differences in experimental conditions, such as methods for visualizing the DNAs and salt concentrations.

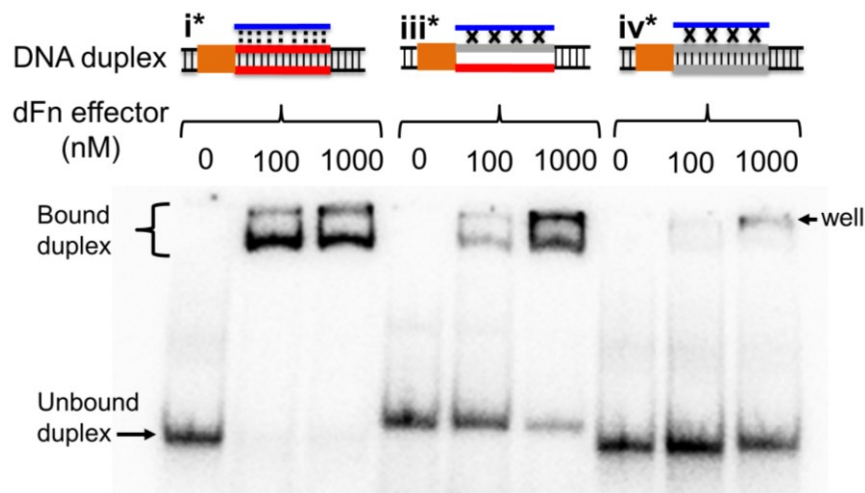


Figure S13: Native gel shift to assess direct binding of DNA with catalytically in-active FnCas12a (dFnCas12a). Data shown were obtained with ³²P-labeled DNA duplex (1 nM) and two concentrations of the dFnCas12a/FnRNA-a effector. DNA duplexes were assembled with the dCas12a/RNA effector in the cleavage reaction buffer following procedures described in Methods (i.e., “DNA cleavage assay”). Upon incubation at 37°C for 30 minutes, equal volume of native loading dye solution (50% glycerol, 0.1% bromophenol blue, 0.1% xylene cyanol, 20 mM Tris pH 7.5, 100 mM KCl, 5 mM MgCl₂) was added, and the sample was then loaded onto an 8% native PAGE. The gel was run at 4°C with the running buffer being 89 mM Tris-HCl, pH 7.5, 89 mM Boric Acid, and 5 mM MgCl₂. The results were visualized by autoradiography. Note that with the presence of the effector, various amount of sample remained in the well. This likely represent DNA bound to the effector, and is considered as “Bound duplex”.

S11. Flexibility of DNA duplexes assessed by site-directed spin labeling

It has been reported that locally “melted” DNA duplexes that contain unpaired nucleotide(s) (i.e., bubbles) are significantly more flexible than fully paired duplexes.⁶ This was verified for DNA duplexes studied in this work using site-directed spin labeling (SDSL). SDSL monitors site-specifically attached stable radicals (e.g., nitroxide spin labels) using Electron Paramagnetic Resonance (EPR) spectroscopy, and provides unique local structural and dynamic information on the parent bio-molecules.⁷ To examine variations in flexibility of DNA duplexes studied in this work, an nt-strand of a DNA substrate was labeled with an R5a nitroxide (Figure S14A)⁸ at selected sites within the protospacer segment, then paired with various t-strand to assemble duplexes with different pairing states at the protospacer segment (Table S3). X-band continuous-wave (cw-) EPR spectra, which report on rotational motion of the nitroxide label, were measured for these duplexes, and the observed spectral lineshapes were analyzed to assess the flexibility of the corresponding DNA duplexes.

Figure S14B shows a representative set of data obtained for duplexes **i** and **iii** (Table S3). Duplex **i**, which has perfect complementarity between the two strands, gave a spectrum with the same characteristics previously reported for R5a-labeled fully-paired DNA duplexes,^{8, 9} with closely spaced splitting at the low-field peak (Figure S14B, indicated by arrows). Prior analyses have revealed that such a low-field splitting pattern arises from an incomplete average of the nitroxide hyperfine interaction, which is the result of anisotropic rotational motions of the R5a nitroxide due to steric confinement at the major groove of a DNA duplex.¹⁰ For duplex **iii**, in which the protospacer segment is unpaired, the observed spectrum shows a relatively sharp low-field peak with no splitting (Figure S14C). This indicates higher nitroxide mobility, which results in a higher degree of averaging of hyperfine interactions. The increase in nitroxide mobility indicates increasing DNA local dynamics at the labeling site, and in turn demonstrates that the unpaired DNA segment does result in higher flexibility in duplex **iii** as compared to duplex **i**. The same results were obtained with the R5a attached at different positions of the protospacer (data not shown). Overall, the data clearly revealed that DNA duplexes with unpaired segment are more flexible than a fully-paired duplex.

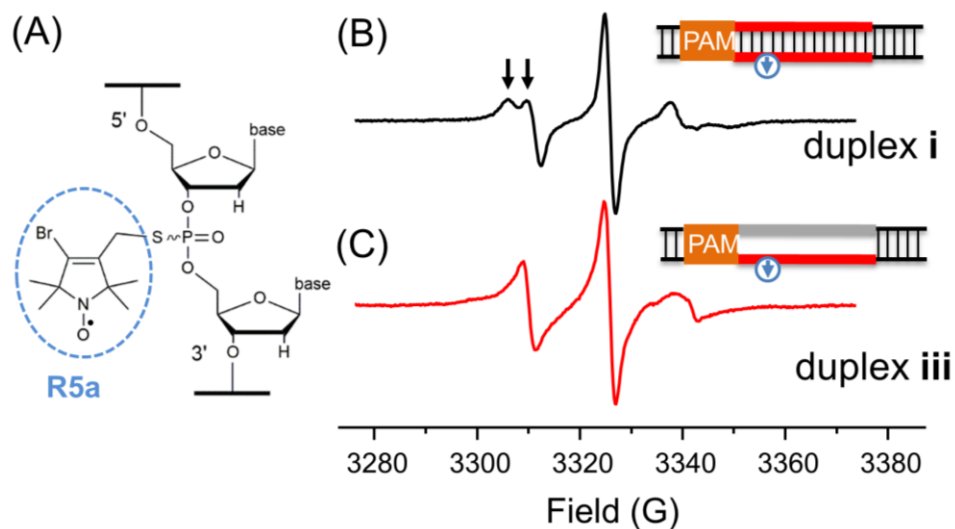


Figure S14. (A) Schematic of the R5a nitroxide label attached to a phosphorothioate within a DNA strand (adapted with permission from Ref. #11; copyright 2017 American Chemical Society). In this work, R5a labeling was carried out following a previously reported protocol.¹¹ A spin labeling reaction (10 μ L) contained 0.1–1 mM crude phosphorothioate-modified oligonucleotide (obtained commercially from Integrated DNA Technologies), 150 mM 3-iodomethyl-1-oxyl-2,2,5,5-tetramethylpyrroline (gift from Kálmán Hideg, University of Pécs, Hungary), 40% (v/v) acetonitrile, and 100 mM 2-(*N*-morpholino)ethanesulfonic acid (MES) pH 5.8. The reaction mixture was incubated at room temperature in the dark with constant mixing for 16–24 hours. Upon conclusion of the reaction, the mixture was subjected to an ethanol precipitation procedure to remove the majority of excess nitroxide precursor. The R5a-labeled DNA strand was assembled into duplexes following procedures described in Methods. Prior to spectral acquisitions, labeled DNA duplexes were subjected to filter concentration to remove the remaining un-attached nitroxide precursor. (B) X-band cw-EPR spectrum of the fully-paired duplex **i**, with an R5a nitroxide (indicated by the blue arrow in the cartoon inset) attached at the PAM+6 phosphate of the nt-strand. The spectrum was acquired at room temperature on a Bruker EMX spectrometer using an ER4119HS cavity. The incident microwave power was 2 mW, and the field modulation was 2 G at a frequency of 100 kHz. The spectrum was acquired with 512 points, corresponding to a spectral range of 100 G, then corrected for background and baseline, and normalized following reported procedures.¹² (C) X-band cw-EPR spectrum of a duplex **iii**, where the protospacer segment is unpaired. The R5a-labeled DNA strand is the same as that in panel (B).

Reference

1. Yamano, T.; Nishimasu, H.; Zetsche, B.; Hirano, H.; Slaymaker, I. M.; Li, Y.; Fedorova, I.; Nakane, T.; Makarova, K. S.; Koonin, E. V.; Ishitani, R.; Zhang, F.; Nureki, O., Crystal Structure of Cpf1 in Complex with Guide RNA and Target DNA. *Cell* **2016**, *165*, 949-62.
2. Zetsche, B.; Gootenberg, J. S.; Abudayyeh, O. O.; Slaymaker, I. M.; Makarova, K. S.; Essletzbichler, P.; Volz, S. E.; Joung, J.; van der Oost, J.; Regev, A.; Koonin, E. V.; Zhang, F., Cpf1 is a single RNA-guided endonuclease of a class 2 CRISPR-Cas system. *Cell* **2015**, *163*, 759-71.
3. Lei, C.; Li, S. Y.; Liu, J. K.; Zheng, X.; Zhao, G. P.; Wang, J., The CCTL (Cpf1-assisted Cutting and Taq DNA ligase-assisted Ligation) method for efficient editing of large DNA constructs in vitro. *Nucleic Acids Res* **2017**, *45*, e74.
4. Stella, S.; Alcon, P.; Montoya, G., Structure of the Cpf1 endonuclease R-loop complex after target DNA cleavage. *Nature* **2017**, *546*, 559-563.
5. Singh, D.; Mallon, J.; Poddar, A.; Wang, Y.; Tippiana, R.; Yang, O.; Bailey, S.; Ha, T., Real-time observation of DNA target interrogation and product release by the RNA-guided endonuclease CRISPR Cpf1 (Cas12a). *Proc Natl Acad Sci* **2018**, *115*, 5444-5449.
6. Forties, R. A.; Bundschuh, R.; Poirier, M. G., The flexibility of locally melted DNA. *Nucleic Acids Res.* **2009**, *37*, 4580-4586.
7. Sowa, G. Z.; Qin, P. Z., Site-directed Spin Labeling Studies on Nucleic Acid Structure and Dynamics. In *Prog Nucleic Acid Res Mol Biol.*, Conn, P. M., Ed. Academic Press: 2008; Vol. 82, 147-197.
8. Popova, A. M.; Kálai, T.; Hideg, K.; Qin, P. Z., Site-Specific DNA Structural and Dynamic Features Revealed by Nucleotide-Independent Nitroxide Probes. *Biochemistry* **2009**, *48*, 8540-8550.
9. Ding, Y.; Zhang, X.; Tham, K. W.; Qin, P. Z., Experimental mapping of DNA duplex shape enabled by global lineshape analyses of a nucleotide-independent nitroxide probe. *Nucleic Acids Res.* **2014**, *42*, e140-e140.
10. Popova, A. M.; Qin, P. Z., A Nucleotide-Independent Nitroxide Probe Reports on Site-Specific Stereomeric Environment in DNA. *Biophys. J* **2010**, *99*, 2180-2189.
11. Tangprasertchai, N. S.; Di Felice, R.; Zhang, X.; Slaymaker, I. M.; Vazquez Reyes, C.; Jiang, W.; Rohs, R.; Qin, P. Z., CRISPR-Cas9 Mediated DNA Unwinding Detected Using Site-Directed Spin Labeling. *ACS Chem. Biol.* **2017**, *12*, 1489-1493.
12. Zhang, X.; Cekan, P.; Sigurdsson, S. T.; Qin, P. Z., Studying RNA using site-directed spin-labeling and continuous-wave electron paramagnetic resonance spectroscopy. *Method Enzymol.* **2009**, *469*, 303-328.